Mon. Not. R. Astron. Soc. **312**, 211–216 (2000)

Observations of OH 4765-MHz maser emission from star-forming regions

M. Szymczak, A. J. Kus and G. Hrynek

Toruń Centre for Astronomy, Nicolaus Copernicus University, ul. Gagarina 11, PL-87100 Toruń, Poland

Accepted 1999 September 21. Received 1999 June 16; in original form 1999 March 16

ABSTRACT

We report observations of the 4765-MHz maser transition of OH ($^2\Pi_{1/2}$, $J = 1/2$, $F = 1 \rightarrow 0$) towards 57 star-forming regions, taken with the 32-m Toruń telescope. Nine maser sources were detected, of which two had not been reported previously. The newly discovered sources in W75N and Cep A and four previously known sources were monitored over periods ranging from a few weeks to six months. Significant variations of the maser intensity occurred on time-scales of one week to two months. The relationships between the flux density and the linewidth for the new sources, established during the rise and fall phases of bursts that lasted 6–8 weeks, are consistent with a model of saturated masers.

Key words: masers – stars: formation – ISM: molecules – radio lines: ISM.

1 INTRODUCTION

The hyperfine transitions of OH in the excited state $^2\Pi_{1/2}$, $J = 1/2$ at 6 cm are generally found in association with compact H II regions and other indicators of star formation, such as molecular outflows and bright far-infrared sources (Zuckerman et al. 1968; Gardner & Ribes 1971; Rickard, Zuckerman & Palmer 1975; Gardner & Martin-Pintado 1983; Cohen, Masheder & Walker 1991; Cohen, Masheder & Caswell 1995). The $F = 1 \rightarrow 1$ main line at 4750.656 MHz and the $F = 1 \rightarrow 0$ and $F = 0 \rightarrow 1$ satellite lines at 4765.562 and 4660.242 MHz, respectively, are seen in broad quasi-thermal emission. The latter line is also visible in absorption in a few sources. The 4765-MHz emission is often accompanied by narrow maser features (Gardner & Martin-Pintado 1983). In the archetypal source W3(OH), the spatial extent of the 4765-MHz maser components is comparable to that for low-surface-brightness emission at 4751 MHz and absorption at 4660 MHz (Gardner, Whiteoak & Palmer 1983; Guilloteau, Baudry & Walmsley 1985; Baudry et al. 1988). Furthermore, the angular sizes of the OH 4.7-GHz masers are similar to those of other OH masers at 1.6 and 6 GHz (Baudry et al. 1988).

Observational characteristics of the excited 4.7-GHz masers differ from those of the ground state 1.6-GHz masers in several ways. The intensity of the excited emission is commonly much weaker (more than two orders of magnitude in several cases) than that of the dominant 1665-MHz line. The spectrum of the 4.7-GHz maser line usually consists of a single narrow unpolarized feature. The excited masers are much more variable than 1.6-GHz masers (Cohen et al. 1991, 1995). On the other hand, 4765-MHz masers are strongly associated with 1720-MHz masers (Palmer, Gardner & Whiteoak 1984). Such an association is achieved in flowing material at a molecular hydrogen density of $10^7\,\mathrm{cm}^{-3}$, a kinetic temperature higher than 100 K and an OH number density of about $10\,\mathrm{cm}^{-3}$ (Gray, Field & Doel 1992). Nevertheless, some model parameters are quite broadly constrained, so more observational data may be useful to refine theoretical models. Unfortunately, OH 4.7-GHz maser sources are very scarce. Although the survey of the bright *IRAS* sources by Cohen et al. (1991, 1995) resulted in an increase of the number of 4.7-GHz masers by 50 per cent, only 19 maser sources have been reported to date. Out of the 15 maser sources with *IRAS* counterparts observed in all three lines, 14 sources are 4765-MHz masers; maser emission for the other transitions are found in only three sources (Cohen et al. 1995). Because the excited maser emission shows considerable intensity variations (Cohen et al. 1991, 1995) or even powerful flares (Smits, Cohen & Hutawarakorn 1998) one can expect to find more 4765-MHz maser sources when monitoring bright far-infrared sources. To check this we have undertaken a survey of the 4765-MHz line in a sample of star-forming regions.

Time-variability properties of 4765-MHz sources have usually been inferred from comparisons of data obtained at epochs spanning 0.5–2 yr (Baudry et al. 1988; Cohen et al. 1995). Recently, Smits et al. (1998) reported variations of the 4765-MHz maser in Mon R2 over a 3-yr period observed on a weekly or fortnightly basis. This source showed unprecedented flaring activity with the flux density variations of an order of magnitude and a shortest time-scale of only 19 days to double in intensity. Observations of maser variability may offer important information to understand effects of saturation in OH maser regions (Gray et al. 1992). In this paper we report the results of 4765-MHz monitoring of newly detected sources together with some already known objects.

2 OBSERVATIONS

The observations were carried out in sessions between 1998 June and December with the 32-m Toruń telescope, which had a half-power beamwidth of 7.5 arcmin at 4.7 GHz. The pointing accuracy was better than 25 arcsec. The telescope was equipped with a cooled HEMT dual-channel receiver accepting opposite circular

Table 1. Observed 4765-MHz OH maser emission.

Name	RA(1950) ($^{h\ m\ s}$)	Dec(1950) ($^{\circ\ \prime\ \prime\prime}$)	Obs. date	V_p (km s^{-1})	$S_p(1\sigma)$ (Jy)	S_i (Jy km s^{-1})
IRAS 02219+6152	02 21 57.0	61 51 30	98.08.17		(0.67)	
(W3-IRS5)			98.11.22		(0.91)	
			98.12.19		(0.70)	
IRAS 02232+6138	02 23 13.7	61 38 46	98.05.29	−44.9	3.71(0.65)	5.41
(W3OH)				−43.2	2.68(0.65)	
			98.07.04	−44.8	4.40(0.86)	4.64
				−43.0	2.93(0.86)	
			98.07.15	−44.9	3.92(0.41)	4.66
				−43.5	1.81(0.41)	
			98.08.16	−44.8	4.38(0.58)	4.64
				−43.1	1.89(0.58)	
			98.10.22	−45.0	4.46(0.78)	4.57
				−43.2	2.43(0.78)	
			98.11.20	−45.1	4.18(0.62)	4.16
				−43.2	1.96(0.62)	
			98.12.02	−44.9	3.94(0.59)	4.81
				−43.1	1.87(0.59)	
IRAS 06053−0622	06 05 20.4	−06 22 31	98.06.30	10.6	5.95(0.84)	3.33
(Mon R2)			98.07.04	10.7	4.37(0.89)	4.04
			98.07.08	10.6	6.20(0.93)	2.79
W49N	19 07 49.8	09 01 17	98.07.05	8.2	3.54(0.92)	1.56
W51	19 21 26.2	14 24 44	98.07.04	58.9	2.09(0.62)	4.71
IRAS 19598+3324	19 59 50.0	33 24 20	98.06.30	−20.4	6.80(1.40)	4.02
(K3-50)			98.10.20	−20.5	2.42(0.75)	2.76
			98.12.01	−20.5	2.23(0.61)	1.69
IRAS 20081+3122	20 08 09.9	31 22 42	98.07.01		(0.55)	
(ON 1)						
W75N[a]	20 36 50.5	42 27 01	98.08.14	10.4	2.91(0.70)	2.75
			98.11.20	10.3	4.29(0.50)	2.82
			98.12.02	10.3	6.11(0.58)	3.65
			98.12.19	10.4	9.95(0.56)	4.47
DR21(OH)	20 37 13.7	42 12 08	98.06.30	−4.0	2.11(0.62)	4.21
				5.2	5.41(0.62)	
IRAS 21413+5442	21 41 21.2	54 42 30	98.07.11		(0.39)	
			98.10.25		(0.84)	
IRAS 22543+6145[a]	22 54 20.2	61 45 55	98.07.03	−14.7	3.40(0.55)	3.94
(Cep A)			98.07.07	−14.8	4.04(0.58)	2.79
			98.07.08	−14.7	5.97(0.69)	3.51
			98.07.14	−14.7	4.47(0.35)	2.51
			98.07.19	−14.6	1.64(0.55)	2.24
			98.07.31	−14.8	2.62(0.75)	2.31
			98.09.22	−14.8	8.06(1.18)	4.65
			98.10.16	−14.6	13.32(0.96)	11.98
			98.10.17	−14.8	10.48(0.72)	7.02
			98.10.19	−14.7	10.44(1.22)	9.41
			98.10.21	−14.7	7.08(0.58)	5.29
			98.10.24	−14.8	6.39(1.00)	5.75
			98.11.20	−14.8	3.36(0.60)	3.54
			98.12.05	−14.9	2.77(0.70)	3.03
			98.12.10	−14.8	3.22(0.74)	1.99
			98.12.15	−14.7	3.86(0.97)	3.10
			98.12.29	−14.6	2.80(0.51)	1.40
IRAS 23116+6111	23 11 36.9	61 11 57	98.07.04	−57.3	3.43(0.92)	3.75
(NGC 7538)			98.10.18	−61.5	1.72(0.67)	3.00
				−57.4	2.28(0.67)	
			98.11.20	−57.1	2.08(0.61)	1.21
			98.12.14	−57.2	3.03(0.85)	1.72

[a]New detection.

polarizations. The system temperature was 45 K on cold sky. The ratio of unpolarized flux density to antenna temperature for the telescope was 6.5 Jy K^{-1}. A two-level autocorrelator, consisting of one bank of 512 channels, was used as the backend. It has a bandwidth of 1 MHz but only the central most sensitive part was used, resulting in an effective velocity span of 52 km s^{-1} and a velocity resolution of 0.25 km s^{-1} after Hanning smoothing. The bulk of the observations were made in left circular polarization. The data were acquired in total-power position switching mode with 15-min on-source integrations interspersed with 15-min integrations on nearby reference positions. The spectra were calibrated by injecting a signal from a noise diode of known temperature at the beginning of each scan. Continuum measurements of the extragalactic sources 3C123 and Vir A, with flux densities from Ott et al. (1994), were used to calibrate the noise diode. The resulting accuracy of the absolute flux density was about 10 per cent. An extensive calibration programme, which was completed before our survey, has shown the 32-m antenna gain reduction at low elevation angle to be less than 2 per cent (Katarzyński 1997). Thus, no elevation-dependent gain correction was applied to our data. The data were processed off-line using the spectral-line analysis package (SLAP). The instrumental baseline was removed by subtracting a first or second order polynomial. The final spectra were obtained by adding a few 15-min scans yielding the rms noise level of about 0.7 Jy.

We selected molecular clouds most of which are sites of recent star formation accompanied by OH 18-cm and H_2O 1.35-cm masers. They are bright far-infrared objects with *IRAS* flux densities greater than 1000 Jy at 60 and 100 μm. In our list of targets there are 33 sources searched for OH 6-cm emission by Cohen et al. (1991, 1995), 18 sources searched for OH 5-cm emission (Baudry et al. 1997) and six strong (peak flux density >250 Jy) H_2O masers at 22 GHz (Wouterloot, Brand & Fiegle 1993).

3 RESULTS

Out of the 57 sources that we observed, the OH 4765-MHz maser emission was detected in nine objects, of which two are new detections. Properties of observed masers are listed in Table 1. For each source, the positions, the epoch, the velocity of the peak emission V_p relative to the local standard of rest, the peak flux density S_p together with the 1σ noise level and the integrated flux density S_i are given. The spectra of the newly detected lines from W75N and Cep A are shown in Fig. 1. The OH 4765-MHz maser from W75N was detected during our first session on 14 August 1998 with a peak flux density of 2.9 Jy at 10.4 km s^{-1}. No search for emission at the other two transitions of the $^2\Pi_{1/2}$ J = 1/2 state was performed. The first observation of Cep A was made on 1998 July 3. A single 4765-MHz maser feature with a peak flux density of 3.0 Jy was found at -14.8 km s^{-1}. At the same epoch Cep A was searched for 4751- and 4660-MHz lines over a velocity range of $-32 - 20$ km s^{-1} but no emission was found to our 3σ upper limit of 1.8 Jy.

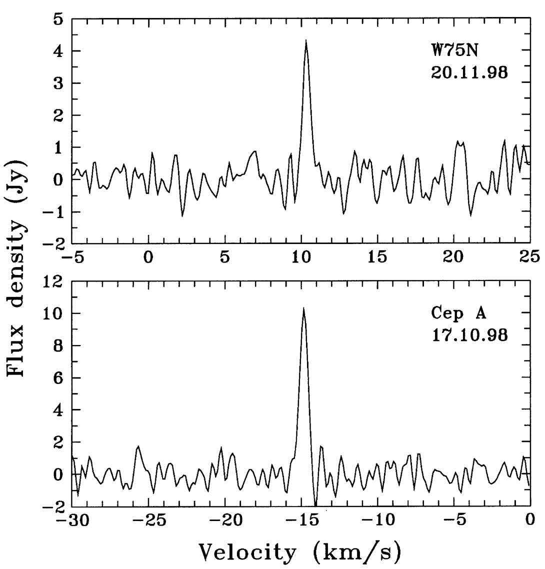

Figure 1. Spectra of newly found OH 4765-MHz masers. Velocities are relative to the local standard of rest. The velocity resolution is 0.25 km s^{-1}.

The non-detections are listed in Table 2 with the positions, the epoch, the velocity interval searched and the 1σ flux density level.

Time variations of the S_p and S_i of the six sources were studied over periods ranging from a few weeks to six months (Table 1). Two new sources showed strong variations by at least a factor of 3. Three sources exhibited moderate variations of about 30 per cent, and one did not vary significantly.

4 INDIVIDUAL SOURCES

4.1 IRAS 02219+6152(W3-IRS5)

A maser feature of about 2 Jy at -37.4 km s^{-1} was observed (Rickard et al. 1975; Gardner et al. 1983). The peak flux density of 1.6 Jy was reported by Cohen et al. (1995). We did not detect it at three occasions with our sensitivity limit of 2.1 Jy.

4.2 IRAS 02232+6138(W3(OH))

The two features of W3(OH) having radial velocities -44.9 and -43.2 km s^{-1} did not vary within 1σ of an average value of 0.6 Jy over a six-month period. Also, no significant variations were recognized in the integrated flux density. Our data extend previous results (Gardner & Martin-Pintado 1983; Baudry et al. 1988; Cohen et al. 1995). Comparison with earlier spectra (Zuckerman et al. 1968; Baudry 1974) shows that the maser intensity and the line shape remain essentially unchanged for a period of 30 yr.

4.3 IRAS 06053−0622(Mon R2)

A strong emission with the peak flux density of ~75 Jy was observed at 1997.5 epoch and afterward by Smits et al. (1998). Our data showed a decrease by at least one order of magnitude. The peak intensity of feature at 10.7 km s^{-1} is still high compared with that observed in 1990 October and 1991 March (Cohen et al. 1995).

4.4 W49N

The feature at 8.2 km s^{-1} only was detected. Its intensity is comparable to that reported by Cohen et al. (1991), while a second feature at 2.2 km s^{-1} lies below our sensitivity limit.

4.5 W51

One maser feature at 57.3 km s^{-1} and a second component at 60.5 km s^{-1} were observed (Gardner & Martin-Pintado 1983). The former feature was confirmed by Cohen et al. (1991), but is below our sensitivity limit. A new feature appeared at 58.9 km s^{-1}.

4.6 IRAS 19598+3324(K3-50)

The flux of the previously known feature at -20.5 km s^{-1} was slightly increased as compared with that reported by Cohen et al. (1991, 1995). We note a decrease of the intensity by a factor of about 2.5 over the 5-month interval of our measurements. Masers at 6031 and 6035 MHz have similar velocities (Baudry et al. 1997).

Table 2. Objects without OH 4765-MHz maser emission.

Name	RA(1950) ($^{h\ m\ s}$)	Dec(1950) ($^{\circ\ \prime\ \prime\prime}$)	Obs. date	Vel. range ($km\,s^{-1}$)	1σ (Jy)
IRAS 02044+6031	02 04 29.0	60 31 42	98.09.25	−80,−28	0.83
IRAS 02236+6142	02 23 37.7	61 42 03	98.10.24	−42,10	0.98
IRAS 02575+6017	02 57 35.6	60 17 21	98.10.24	−60,−8	0.86
IRAS 02589+6014	02 58 56.3	60 14 10	98.10.24	−49,3	0.92
IRAS 03035+5819	03 03 33.2	58 19 21	98.10.25	−47,5	0.83
IRAS 03037+5819	03 03 46.7	58 20 00	98.10.25	−39,13	0.98
IRAS 03236+5836	03 23 38.6	58 36 38	98.08.08	−40,12	0.65
			98.12.20	−40,12	0.71
IRAS 03245+3002	03 24 34.0	30 02 36	98.08.06	−27,25	0.74
IRAS 04361+2547	04 36 09.8	25 47 41	98.08.12	−22,30	0.63
Ori-IR	05 32 47.0	−05 24 23	98.06.01	−18,34	1.21
IRAS 05358+3543	05 35 48.8	35 43 10	98.08.01	−46,7	0.62
IRAS 05387−0149	05 38 47.7	−01 49 00	98.10.21	−68,−18	0.80
IRAS 05391−0152	05 39 07.1	−01 52 45	98.10.22	−30,22	0.92
IRAS 05392−0214	05 39 13.7	−02 14 48	98.12.15	−28,24	0.84
IRAS 05445+0020	05 44 31.3	00 20 48	98.08.13	−14,38	1.14
IRAS 06055+2039	06 05 33.9	20 39 47	98.07.13	−19,33	0.80
			98.07.19	−19,33	0.61
IRAS 06058+2138	06 05 53.7	21 39 09	98.08.01	−22,30	1.00
IRAS 06061+2151	06 06 07.3	21 51 12	98.08.13	−39,13	0.95
IRAS 06084−0611	06 08 25.6	−06 10 49	98.09.06	−19,33	1.02
IRAS 06099+1800	06 09 58.2	18 00 17	98.09.07	−23,29	0.78
IRAS 06117+1350	06 11 46.3	13 50 31	98.09.05	−9,43	1.00
IRAS 18274+0112	18 27 25.0	01 12 40	98.10.20	−20,32	0.96
IRAS 18403−0417	18 40 19.5	−04 17 01	98.12.03	68,120	0.72
IRAS 18411−0338	18 41 07.9	−03 38 41	98.09.06	66,118	0.92
IRAS 18434−0242	18 43 24.6	−02 42 48	98.09.05	65,117	1.00
IRAS 18449−0115	18 44 59.5	−01 16 07	98.09.05	70,122	0.99
	18 45 11.0	−01 57 57	98.08.16	70,122	0.80
IRAS 18487−0015	18 48 47.9	−00 15 46	98.12.06	5,57	0.52
IRAS 18507+0110	18 50 46.9	01 10 49	98.12.05	35,87	0.49
IRAS 18515+0157	18 51 32.7	01 57 45	98.07.10	18,70	0.56
IRAS 18556+0136	18 55 41.2	01 36 28	98.12.12	13,65	0.39
IRAS 19095+0930	19 09 31.2	09 30 51	98.07.03	15,67	1.01
			98.12.17	15,67	0.64
IRAS 19111+1048	19 11 06.2	10 48 23	98.12.17	42,94	0.91
			98.12.23	42,94	0.54
IRAS 19120+1103	19 12 00.4	11 03 59	98.12.13	28,80	0.61
IRAS 19181+1349	19 18 13.0	13 49 44	98.08.15	5,52	0.96
IRAS 19446+2505	19 44 41.9	25 05 30	98.08.14	0,52	0.87
ON2	20 19 50.5	37 16 30	98.07.05	−33,19	0.80
IRAS 20198+3716	20 19 48.9	37 15 52	98.08.07	−34,18	0.72
IRAS 20255+3712	20 25 32.8	37 12 54	98.07.12	−42,10	0.98
			98.09.06	−42,10	0.86
IRAS 20275+4001	20 27 36.0	40 01 16	98.08.01	−39,13	0.88
IRAS 20350+4126	20 35 04.8	41 26 02	98.12.05	−41,11	0.64
IRAS 21144+5430	21 14 24.1	54 30 57	98.12.20	−116,−64	0.65
IRAS 21306+5540	21 30 37.1	55 40 05	98.12.23	−110,−58	0.69
IRAS 22176+6303	22 17 41.2	63 03 43	98.07.18	−37,15	0.51
			98.08.16	−37,15	0.77
IRAS 22198+6336	22 19 50.7	63 36 33	98.12.23	−48,4	0.73
IRAS 22566+5830	22 56 38.3	58 30 52	98.07.10	−78,−26	0.60
			98.12.06	−78,−26	0.47
			98.12.23	−78,−26	0.51

4.7 IRAS 20081+3122(ON 1)

The features at $9.5\,km\,s^{-1}$ (Baudry 1974) and at $24.1\,km\,s^{-1}$ (Gardner & Martin-Pintado 1983) of similar intensity of about 2.2 Jy were not detected in 1998 with our sensitivity limit of 1.6 Jy. The emission was not detected in 1989, 1990 and 1991 to a limit of 0.27 Jy (Cohen et al. 1991, 1995).

4.8 W75N

Between 1998 August and December the S_p of W75N increased from 2.9 to 9.9 Jy, while the S_i increased by a factor of 2. A significant rise of S_p by a factor of 2 occurred during the last month of our observations. The linewidth (full width at half intensity) of the maser feature of W75N decreased during the observing period from 0.36 to $0.18\,km\,s^{-1}$. The velocity of the excited maser is similar to that of the strongest 1665-MHz maser feature seen in 1976 (Haschick et al. 1981). No 4765-MHz maser emission was detected in 1989 with a sensitivity limit of 0.22 Jy (Cohen et al. 1991). Rickard et al. (1975) reported the excited OH maser emission at 6035 MHz. This emission ranges from 6.7 to $8.2\,km\,s^{-1}$ (Baudry et al. 1997).

4.9 DR21(OH)

This source was reported as a variable 4765-MHz maser with a double profile (Cohen et al. 1991, 1995). Our measurements show that the emission is essentially the same as that which was observed in 1989 (Cohen et al. 1991). Three weak maser features at 6035 MHz were found by Baudry et al. (1997) in the velocity range from -8.8 to $-2.1\,\mathrm{km\,s^{-1}}$.

4.10 IRAS 21413+5442

The weak emission of 0.7 Jy detected by Cohen et al. (1991) lies below our 3σ detection limit.

4.11 IRAS 22543+6145(Cep A)

This new discovery at 4765 MHz is one of the strongest sources detected. The excited OH emission towards Cep A was observed on 17 occasions. Changes in S_p by a factor of 2 appeared on the time-scale of a week. By 1998 October 16 the peak flux increased to 13.3 Jy and decreased to 6.4 Jy after 8 days. Cohen et al. (1991) did not detect masers 11 yr earlier in all three 4.7-GHz lines with a sensitivity limit of about 0.30 Jy. The maser feature at a velocity of $-14.8\,\mathrm{km\,s^{-1}}$ lies close to the strongest 1665-MHz line observed in 1986 (Migenes, Cohen & Brebner 1992). Weak excited masers at 6035 and 6031 MHz detected in 1995 by Baudry et al. (1997) range from -10.1 to $-8.6\,\mathrm{km\,s^{-1}}$.

4.12 IRAS 23116+6111(NGC7538)

At least three maser features (0.2–0.3 Jy) in the velocity range from -57.1 to $-59.2\,\mathrm{km\,s^{-1}}$ were observed in 1982 (Gardner & Martin-Pintado 1983; Palmer et al. 1984), but lie below our 3σ upper limit. No emission was detected in 1989 to a limit of 0.26 Jy (Cohen et al. 1991). After two years, a single feature of 0.7 Jy at $-59.2\,\mathrm{km\,s^{-1}}$ was observed by Cohen et al. (1995). We detected a feature at $-57.2\,\mathrm{km\,s^{-1}}$, which persisted over six months of our monitoring. Its flux density had increased by an order of magnitude since it was observed by Gardner & Martin-Pintado (1983) and Palmer et al. (1984). A tentative feature at $-61.5\,\mathrm{km\,s^{-1}}$ was detected on one occasion.

5 DISCUSSION

The present study demonstrates that a moderate sensitivity survey of star-forming regions associated with powerful far-infrared sources can be a useful means of detecting new sources of OH 4765-MHz maser emission. In nine sources, which correspond to 16 per cent of our sample, we find the excited maser line. Five of them are listed in the *IRAS* Point Source Catalog (1985) and their 60-μm flux densities are greater than 7000 Jy. An increase of detection rate of 4.7-GHz masers among the brightest far-infared sources was first noticed by Cohen et al. (1995). However, they did not find any correlation between 4.7-GHz and 60-μm flux densities. Also, there are little differences in the *IRAS* colours of maser and non-maser sources (Cohen et al. 1995).

The newly found OH 4765-MHz sources belong to a small group of well-studied objects associated with continuum emission of compact H II regions and with line emission of several molecules. Though significant changes are observed in maser emission a comparison of available spectra of masing and thermal lines may be of some value to localize the excited 4765-MHz emission in those objects.

W75N is located in a molecular cloud at an average radial velocity near $9\,\mathrm{km\,s^{-1}}$ (Dickel, Dickel & Wilson 1978). The CS $J = 7 \rightarrow 6$ emission, which traces the dense core, peaks at $10\,\mathrm{km\,s^{-1}}$ (Hunter et al. 1994). The $C^{18}O$, $J = 2 \rightarrow 1$ line peaks at the same velocity (Jaffe et al. 1989). The OH 1665-MHz maser emission ranges from 3.2 to $13.2\,\mathrm{km\,s^{-1}}$ (Haschick et al. 1981; Baart et al. 1986). The strongest emission appears at $12\,\mathrm{km\,s^{-1}}$, while at $10.4\,\mathrm{km\,s^{-1}}$ only weak (about 0.6 Jy) emission was detected with MERLIN (Baart et al. 1986). The H_2O maser spectrum extends over $30\,\mathrm{km\,s^{-1}}$ with the strongest feature near $12\,\mathrm{km\,s^{-1}}$ (Hunter et al. 1994). We note that the OH 4765-MHz emission appears at essentially the same velocity as the CS core emission, while the strong OH maser emission at other transitions is shifted in velocity by ± 2–$3\,\mathrm{km\,s^{-1}}$. This suggests that excited OH emission may arise near the core of the object.

CO $J = 3 \rightarrow 2$ emission towards Cep A has a total velocity extent of about $45\,\mathrm{km\,s^{-1}}$ (Narayanan & Walker 1996). The CS $J = 7 \rightarrow 6$ line peaks near $-12\,\mathrm{km\,s^{-1}}$ which is close to the central velocity of CO line. We state that the 4765-MHz emission is blueshifted by $\sim 3\,\mathrm{km\,s^{-1}}$ relative to the CS emission. The OH masers at 1665 and 1667 MHz range from -17 to $0\,\mathrm{km\,s^{-1}}$ (Migenes et al. 1992). The bright components identifiable at several epochs appear at -16 to $-14\,\mathrm{km\,s^{-1}}$ where we found the excited maser emission.

The above analysis of the radial velocities at different transitions suggests that at least for W75N the excited OH 4765-MHz masers come from regions located near the core of the source. This appears to be consistent with the model by Gray et al. (1992) where 4765-MHz masers operate in hot and dense medium, which has the kinetic temperature $T_\mathrm{K} = 125\,\mathrm{K}$ and the molecular hydrogen density $n = 2 \times 10^7\,\mathrm{cm^{-3}}$. The 1665-MHz masers are predicted at velocities shifted by $3\,\mathrm{km\,s^{-1}}$ in regions with $T_\mathrm{K} = 60\,\mathrm{K}$ and $n = 7 \times 10^6\,\mathrm{cm^{-3}}$ (Gray et al. 1992). High-angular-resolution measurements of the new sources are required to determine the location of excited masers.

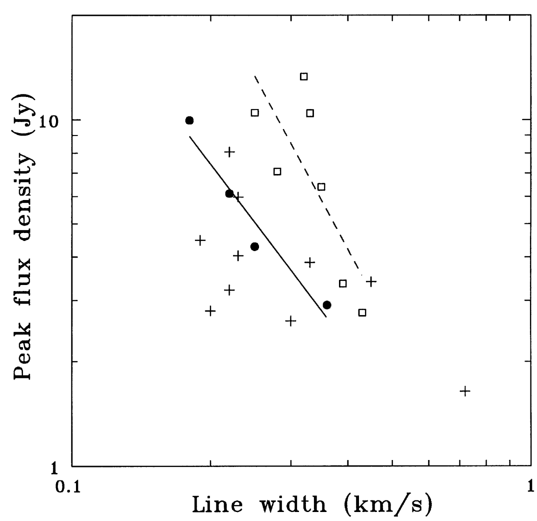

Figure 2. Plot of the peak flux density against the linewidth for the 4765-MHz maser line outburst in W75N (filled circles) and in Cep A after the maximum (open squares); the best least-squares fits for the data are shown by a solid and dashed line, respectively. Measurements of Cep A before maximum and during a quiescent period are marked by crosses.

The 4765-MHz masers are generally highly variable. Time-scales of variability ranging from a few weeks to several years have been reported previously (Gardner & Martin-Pintado 1983; Cohen et al. 1995; Smits et al. 1998). The present data provide information on the variability of the 4765-MHz masers with intervals from a few weeks to six months. Comparison of our data with those of Cohen et al. (1991) shows that between 1989 and 1998 the maser intensities from W75N and Cep A must have increased by at least one order of magnitude with time intervals as short as a few days of significant variations in the maser intensity. On 1998 October the peak intensity of emission from Cep A reached a maximum. Because the flux density was poorly sampled just before maximum, we can only deduce that a decay time was about 1.5 months. The maser intensity in W75N showed a gradual increase during four consecutive epochs. If there are no blended features in the 4765-MHz spectra, then the intensity variations must be intrinsic to the line.

In Fig. 2 the peak flux density S_p against the linewidth (full width at half maximum) ΔV is plotted for both sources. The W75N data marked by filled circles are fitted by a solid line. For Cep A, the measurements after maximum at 1998.79 indicated by squares are fitted by a dashed line, while crosses mark the rest of the data obtained during a quiescent period. The slope of both lines indicates that $\Delta V \sim S_p^{\alpha}$, where α is -0.57 ± 0.06 and -0.40 ± 0.11 for W75N and Cep A, respectively. We interpret these relationships using the standard maser theory (Goldreich & Kwan 1974). During unsaturated growth $\Delta V \sim \tau^{-0.5}$, where τ is the opacity in the maser line. When the effect of infrared photon trapping is taken into account, the same law works for saturated amplification. Because for saturated masers $S_p \sim \tau$, we obtain $\Delta V \sim S_p^{-0.5}$. Therefore, we can conclude that the outburst variations of the linewidth during a presumably rising phase in W75N and the decay phase in Cep A are consistent with a model of saturated masers. Data with better time resolution may allow us to determine precisely the degree of saturation.

One sees from the calculations of Gray et al. (1992), for the model with $T_K = 125\,K$, $n = 2 \times 10^6\,cm^{-3}$ and the OH number density $n_{OH} = 2 \times 10^2\,cm^{-3}$, that the 4765-MHz maser saturates when $\tau \geq 11$ and the unsaturated maser gain length is about 10^{14} cm. This value of opacity in the line appears to be consistent with that discussed by Baudry et al. (1988). Using high-angular-resolution data, they provided arguments supporting a view that at least the strongest 4765-MHz masers in W3(OH) are saturated. Our data confirm a previous finding that the maser emission from W3(OH) is stable in time (Baudry et al. 1988); we argue that a general level of maser emission has been maintained for up to 30 yr. In this respect, W3(OH) appears to be a peculiar source. The rest of the OH sources in our sample have intensities that differed by a factor of a few from measurements taken 11 years ago (Cohen et al. 1991). Rapid variations of maser features may indicate unsaturated growths and decays of stimulated emission.

6 CONCLUSIONS

The 32-m Toruń telescope survey of the OH 4765-MHz maser emission in selected star-forming regions resulted in the detection of nine sources, of which two were detected for the first time. The OH sources are preferentially associated with the bright far-infrared sources. Six sources were monitored in the time intervals from a few weeks to six months. Significant variations of the maser emission on time-scales of 6–8 weeks were detected. Changes of the linewidth with the maser intensity during the rise and fall periods of bursts in W75N and Cep A are consistent with a model of saturated emission. The radial velocities of the excited 4765-MHz emission in those sources are quite near to the velocities of the CO and CS thermal lines. High-resolution data are needed to examine the location of maser acitivity centres.

REFERENCES

Baart E. E., Cohen R. J., Davies R. D., Norris R. P., Rowland P. R., 1986, MNRAS, 219, 145
Baudry A., 1974, A&A, 33, 381
Baudry A., Diamond P. J., Booth R. S., Graham D., Walmsley C. M., 1988, A&A, 201, 105
Baudry A., Desmurs J. F., Wilson T. L., Cohen R. J., 1997, A&A, 325, 255
Cohen R. J., Masheder M. R. W., Walker R. N. F., 1991, MNRAS, 250, 611
Cohen R. J., Masheder M. R. W., Caswell J. L., 1995, MNRAS, 274, 808
Dickel J. R., Dickel H. R., Wilson W. J., 1978, ApJ, 223, 840
Gardner F. F., Martin-Pintado J., 1983, A&A, 121, 265
Gardner F. F., Ribes J. C., 1971, Astrophys. Lett., 9, 175
Gardner F. F., Whiteoak J. B., Palmer P., 1983, MNRAS, 205, 297
Goldreich P., Kwan J., 1974, ApJ, 190, 27
Gray M. D., Field D., Doel R. C., 1992, A&A, 262, 555
Guilloteau S., Baudry A., Walmsley C. M., 1985, A&A, 153, 179
Haschick A. D., Reid M. J., Burke B. F., Moran J. M., Miller G., 1981, ApJ, 244, 76
Hunter T. R., Taylor G. B., Felli M., Tofani G., 1994, A&A, 284, 215
Jaffe D. T., Genzel R., Harris A. I., Lugten J. B., Stacey G. J., Stutzki J., 1989, ApJ, 344, 265
Joint IRAS Working Group 1985, IRAS Point Source Catalog. U.S. GPO, Washington, DC
Katarzyński K., 1997, MSc thesis, Nicolaus Copernicus University
Migenes V., Cohen R. J., Brebner G. C., 1992, MNRAS, 254, 501
Narayanan G., Walker C. K., 1996, ApJ, 466, 844
Ott M., Witzel A., Quirrenbach A., Krichbaum T. P., Standke K. J., Schalinski G. J., Hummel C. A., 1994, A&A, 284, 331
Palmer P., Gardner F. F., Whiteoak J. B., 1984, MNRAS, 211, 41P
Rickard L. J., Zuckerman B., Palmer P., 1975, ApJ, 200, 6
Smits D. P., Cohen R. J., Hutawarakorn B., 1998, MNRAS, 296, L11
Wouterloot J. G. A., Brand J., Fiegle K., 1993, A&AS, 98, 589
Zuckerman B., Palmer P., Penfield H., Lilley A. E., 1968, ApJ, 153, L69

This paper has been typeset from a TEX/LATEX file prepared by the author.